ORIGINAL PAPER

O. Rahbek · S. Kold · B. Zippor · S. Overgaard ·
K. Søballe

Particle migration and gap healing around trabecular metal implants

Abstract Bone on-growth and peri-implant migration of polyethylene particles were studied in an experimental setting using trabecular metal and solid metal implants. Cylindrical implants of trabecular tantalum metal and solid titanium alloy implants with a glass bead blasted surface were inserted either in an exact surgical fit or with a peri-implant gap into a canine knee joint. We used a randomised paired design. Polyethylene particles were injected into the knee joint. In both types of surgical fit we found that the trabecular metal implants had superior bone ongrowth in comparison with solid metal implants (exact fit: 23% vs. 7% [p=0.02], peri-implant gap: 13% vs. 0% [p=0.02]. The number of peri-implant polyethylene particles was significantly reduced around the trabecular metal implants with a peri-implant gap compared with solid implants.

Résumé Dans un cadre expérimental, nous avons étudié la réhabilitation osseuse et la migration péri-implant de particules de polyéthylène en utilisant des implants en métal trabéculaire et des implants en métal massif. Des implants cylindriques de tantale trabéculaire et des implants en alliage de titane massif avec traitement de surface ont été inséré avec une adaptation exacte ou avec un espace péri-implant dans des genoux de chiens. Nous avons utilisé une forme randomisée par paire. Des particules de polyéthylène ont été injectées dans le genou. Dans les deux types d'implantation nous avons trouvé que les implants en métal trabéculaire avaient une réhabilitation osseuse supérieure en comparaison des implants en métal massif. Le nombre de particules de polyéthylène était notablement réduit autour de l'implant en métal trabéculaire avec un intervalle péri-implant comparé aux implants en métal massif.

O. Rahbek (✉) · S. Kold · B. Zippor · K. Søballe
Orthopedic Research Laboratory, Aarhus University Hospital,
Nørrebrogade 44, Building 1A,
8000 Aarhus, Denmark
e-mail: ole_rahbek@mail.dk
Tel.: +45-8-9494134
Fax: +45-8-9494150

O. Rahbek · S. Kold · B. Zippor · K. Søballe
Institute of Experimental Clinical Research,
Aarhus University Hospital,
Brendstrupgårdsvej 100,
8200 Aarhus, Denmark

O. Rahbek · S. Kold · B. Zippor · K. Søballe
Department of Orthopedics, Aarhus University Hospital,
Nørrebrogade 44,
8000 Aarhus, Denmark

S. Overgaard
Department of Orthopedics, Odense University Hospital,
Sdr. Boulevard 29,
5000 Odense, Denmark

Introduction

Trabecular metal represents a new type of implant material and is used for porous monoblock acetabular implants with an integrated polyethylene liner [7]. The potential risk of backside wear is thus eliminated. In an experimental trans-cortical press-fit model, trabecular metal has obtained promising bone ingrowth and mechanical fixation [6]. Furthermore, a canine study has also shown good osseo-integration of acetabular trabecular metal components [7]. However, long-term clinical results of this implant material are lacking. A concern is the permeability of the trabecular implants, which may increase the transportation of wear debris to the bone implant interface compared with implants with a lower porosity and solid substrates. High failure rates due to particle-mediated aseptic loosening might therefore be feared.

This experimental study investigated the influence of trabecular metal on the migration of polyethylene (PE) particles to peri-implant areas of bone. A solid impermeable titanium alloy implant served as control. Two surgical fittings (exact and gap) were applied to mimic the clinical setting, where implants, even though inserted with press fit, initially have large areas without bone–implant contact [14, 20].

It was hypothesised that the open-pored trabecular metal implants would increase the peri-implant level of PE particles by providing access routes to the interface through

the interconnected pores of the implant. The highest level of PE particles was expected in the model with the highest permeability. This was expected to be the trabecular metal (Tm) implants inserted leaving a gap.

Materials and methods

Design

Two implants were implanted in each knee joint of eight dogs. Trabecular metal (Tm) and glass bead-blasted (Gb) implants were inserted in a randomised paired design. In the lateral femoral condyle of the knee joint the implants were inserted as an exact fit. In the medial femoral condyle implants were inserted with a 0.75-mm gap from the trabecular bone. The experimental implants were fixed by a stable loaded implant device [23]. Joint fluid was in contact with the bone–implant interface. Intra-articular injections with PE particles began three weeks after surgery and were performed weekly until the dogs were killed 8 weeks after surgery.

Animals

Eight mongrel dogs weighing 24–30 kg (average 27 kg) were included in this study. The dogs were bred for scientific purposes and were handled according to the Danish law on animal experimentation.

Implants

The implants were cylindrical (length: 9 mm, diameter: 6 mm). The solid titanium alloy (Ti-6-Al-4V) implants had a slightly roughened surface from glass bead blasting. Trabecular metal implants were highly porous and made of pure tantalum. The pore size of the material is an average of 550 μm, which has been experimentally proven to allow good bone ingrowth [6]. The implants were sterilised by gamma irradiation. Analyses for roughness were performed at the Danish Technology Institute and done on two implants of each kind. Four longitudinal measurements were performed on each implant with 90° between the measurements. A stylus with a tip radius of 2 μm without skid was used. The cut-off filter was 0.8 mm and the evaluation length was 4.0 mm per measurement. Mean Ra was 24 μm (SD 3 μm) with R max 137 μm (SD 4 μm) for the two Tm implants. Gb implants (n=2) had a mean Ra of 1.1 μm (SD 1.1 μm) and R max of 8 μm (SD 0 μm). The porosity of the trabecular metal was determined by scanning electron microscopy (SEM) with backscatter mode (Maxim 2040S, CamScan Electron Optics). Analysis was performed on 3-mm thick successive transverse sections of four epoxy embedded Tm implants. Porosity was defined as an area of void spaces (plastic) as a percentage of the total area of ROI and analysis was done by a grey-scale threshold with image analysis software (ImageJ). The mean porosity of Tm implants was 75% (SD 5%).

Characteristics of injected material

The PE powder consisted of 100% pure crystalline high-density polyethylene (HDPE; Shamrock Technologies, from Smith and Nephew Richards, Memphis, TN, USA). SEM (Cambridge S360) had determined the particle size distribution with automatic image analysing equipment [22, 23]. The analysis was performed at the Danish Technological Institute. The mean equivalent circle diameter was 2.09 μm (range 0.2–11) and the shape was spherical. The powder consisted of 7% particles with a diameter below 1 μm.

The particles were gamma-sterilized. Immediately before use, the particles were suspended in sterile hyaluronic acid (1.75 mg hyaluronic acid/ml phosphate-buffered saline, pH 7.4) and mixed in a vial. Hereafter, the vial was placed in an ultrasound bath for 30 min to homogenise the suspension. The suspension contained 5 mg HDPE (approximately 1.2×10^9 particles) per ml hyaluronic acid as in previous studies [22, 23]. The particles and hyaluronic acid were previously analysed by gas chromatography-tandem mass spectrometry. The analysis is highly sensitive to trace levels of lipopolysaccharide (endotoxin) [27]. There were no biochemical markers for endotoxins in any of the samples tested.

Injection procedure of PE particles

Intra-articular injections using sterile technique were started three weeks after surgery and were repeated weekly, a total of five times per dog. The lateral and medial joint chamber of each knee received 2.5 ml injection substance by parapatellar injection (Fig. 1). The dogs were under brief intravenous anesthesia (thiobarbital) during the procedure.
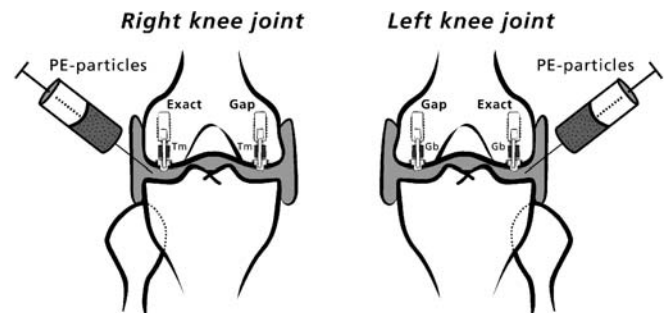
Fig. 1 Design of the study. Two implants were inserted into each knee joint. Trabecular metal (*Tm*) implants or glass bead (*Gb*)-blasted implants were used. The type of implant was randomly alternated between the left and right knees. Implants inserted into the lateral condyles were inserted as an exact fit and implants in medial condyles were inserted with a peri-implant gap. High-density polyethylene particles were injected into both knee joints

Surgical techniques

We used a stable weight-loaded implant device developed by Søballe et al. [26]. The implants were inserted using a sterile technique, while the dogs were under a general inhalatory anesthesia with isoflurane. The knee joints were exposed by the subvastus approach. The patella was dislocated laterally to expose the femoral condyles. Low-speed drilling was performed with K-wire guided cannulated trap drills. Cooling with saline was used to avoid thermal trauma to the bone. Bone debris was washed from the drilled cavity with physiological saline. A 7.5-mm hole was created in the medial femoral condyle leaving a 0.75-mm gap around the 6-mm implants. In the lateral femoral condyle a 6-mm drill hole was created around the implant providing an exact fit as described earlier [21]. A threaded anchorage screw centralised the test implant and a PE plug in the drilled hole. The PE plug (diameter 4.5 mm) protruded slightly above the cartilage so a load was transferred through the implant system at each gait cycle. A titanium ring inserted in the subchondral part of the condyle prevented early tissue ongrowth to the PE plug. A 1.5-mm gap existed between the PE plug and the titanium ring to allow access of joint fluid to the bone–implant interface. The knee was tested after implantation and free motion of the knee joint was ensured. Prophylactic antibiotics (ampicillin) were administrated immediately before surgery. Analgesics (fentanyl plaster) were used for the first three postoperative days. Full weight-bearing was allowed postoperatively.

Specimen preparation

The distal femur was cleared of soft tissue and stored at −20°C immediately after the dogs were killed. Specimens of implants with surrounding bone were prepared with a water-cooled diamond band saw (Exact Appartebau, Norderstedt, Germany). The bone implant specimen was dehydrated in graded ethanol (70–100%) containing basic fuchsin 0.4% and embedded in methylmethacrylate. In accordance with the vertical section method, the implant was randomly rotated around the long axis of the cylindrical implant to obtain random sampling around this axis. Then serial sectioning was performed on a microtome (KDG-95; MeProTech, Heerhugowaard, Netherlands) with 350 µm between sections [3]. Four sections were cut from the central part of each implant. Sections were approximately 35 µm thick and were counterstained with 4% light green [10]. The sections were used to estimate particle migration, tissue ongrowth and gap healing.
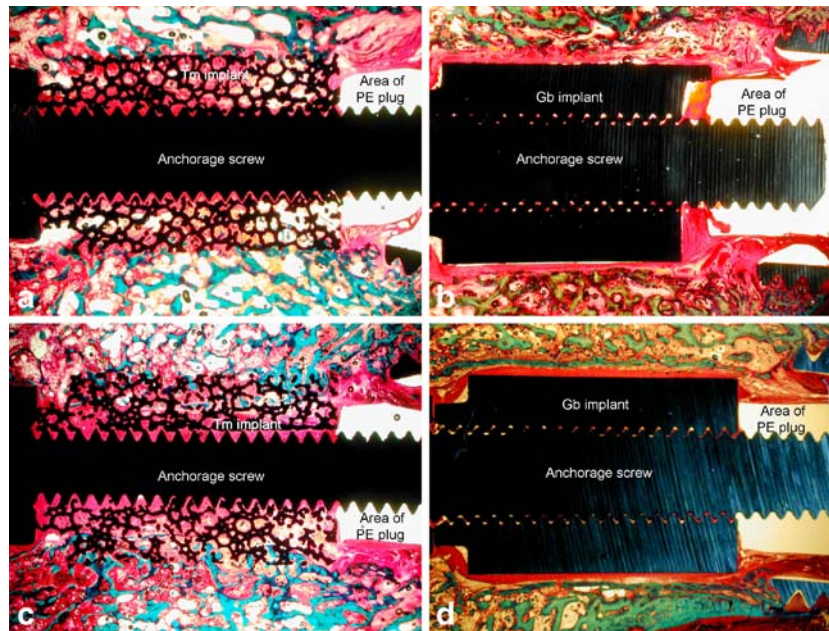
Fig. 2 a–d Histological sections of the four groups. Basic fuchsin stained soft tissue red and light green stained bone green. The polyethylene (PE) plug was removed from the specimens before histological preparation and therefore only the area of the PE plug is indicated on the sections. **a** Tm implant inserted as an exact fit. Bone ingrowth into the implant was present in all peripheral regions of the implant. The inner pores of the implant were mostly filled with fibrous tissue. **b** Gb-blasted implant inserted as an exact fit. The implant was partly covered by a fibrous membrane surrounded by disrupted bone. These findings suggested that bone had been resorbed at the interface and had been replaced by fibrous tissue. The fibrous tissue was in continuity with the fibrous tissue around the PE plug, allowing joint fluid and PE particles access to the peri-implant tissue. **c** Tm implant inserted, with a peri-implant gap. The gap had been bridged by bone formation and ingrowth into the implant was present in all peripheral regions of the implant. However, the inner pores of the implant were mostly filled with fibrous tissue as seen in the group of exactly fitted implants. **d** Gb-blasted implant inserted, with a peri-implant gap. The implant was fully covered by a fibrous membrane. A sclerotic bone rim had formed around the fibrous implants as visible in revision cavities. The fibrous tissue was in continuity with the fibrous tissue around the PE plug as seen in the exact fit implants

Histomorphometry

A stereological software program was applied (CAST-Grid, Olympus Denmark A/S) for histomorphometry. This is based on a user-specified grid or counting frame superimposed on the microscopic fields transmitted to the monitor of a personal computer (attached to a light microscope, objective ×10, ocular ×10). By using the vertical section method [3] and the applied grid systems, it was possible to calculate unbiased estimates by means of stereological methods even though cancellous bone is anisotropic [12, 18]. Four sections were counted per implant to reduce the variance from the section level to a minimum [19].

Migration of PE particles was evaluated by use of a counting frame (700×940 µm) as previously described [22]. Grade 0 was used if no particles were present inside the counting frame. If 1–10, 11–20, 21–50 or over 50 particles were present, grades 1, 2, 3 and 4 were used respectively. The counting frame was aligned to the implant surface and the peri-implant tissue in the range of 700 µm from the surface was analysed. PE particles were identified with polarised light microscopy.

Ongrowth was implant surface in contact with bone, bone marrow, fibro-cartilage or fibrous tissue as a percentage of the total implant surface estimated by the linear intercept technique. The implant surface was defined as the first intersection between the test line and the periphery of the implant. A mean of 307 (range 238–377) intersections were counted per implant.

The 700-µm area adjacent to the implant surface was analysed using a point-counting technique with a mean of 531 (range 357–586) points per implant. The percentages of bone, fibro-cartilage, bone marrow and fibrous tissue were estimated.

Statistics

SPSS 10.0 statistical software was used. Wilcoxon signed rank sum test was used as data did not have a normal distribution. Two tailed p values below 0.05 were considered significant. Median values and range are presented unless otherwise stated.

Table 1 Ongrowth to the implant surface

Ongrowth in percentage		Surgical technique			
		Exact fit	p value	Peri-implant gap	p value
Bone	Gb implants	7 (0–11)	0.02	0 (0–0)	0.02
	Tm implants	23 (19–29)		13 (10–12)	
Fibrous tissue	Gb implants	75 (60–79)	0.02	100 (92–100)	0.02
	Tm implants	5 (1–12)		2 (2–10)	

Gb glass bead-blasted titanium alloy, *Tm* trabecular metal (tantalum)
Median values with interquartile range
Only values for bone and fibrous tissue are given

Table 2 Percentage of bone and fibrous tissue in a 0.7-mm zone adjacent to the implant surface

Volume of peri-implant tissue in percentage		Surgical technique			
		Exact fit	p value	Peri-implant gap	p value
Bone	Gb implants	40 (30–43)	0.87	20 (13–23)	0.06
	Tm implants	36 (27–46)		25 (23–26)	
Fibrous tissue	Gb implants	21 (15–31)	0.02	55 (45–61)	0.02
	Tm implants	4 (0–6)		2 (0–2)	

Median values with interquartile range
Only values for bone and fibrous tissue are given

Results

Animals

One dog was killed 2 days after surgery because it had developed a limp. At autopsy, all implant systems were found to be well placed in the femoral condyles and there was free range of motion of the knees. There were no macroscopic signs of infection. Seven dogs completed the study and were fully weight-bearing on the hind limbs within a week of surgery. Synovitis and excess of joint fluid were found in the knee joints possibly due to a PE particle-induced synovial inflammation as seen in previous studies [22, 23].

Histology

Exact-fitted implants

Trabecular metal implants had superior bone ongrowth with all implants gaining over 18% bone coverage (Fig. 2a, b, Table 1). The maximal bone ongrowth obtained by a Gb implant was 14%. One Gb implant was completely covered by fibrous tissue. Tm and Gb had approximately the same amount of bone volume in the 750-µm zone adjacent to the implant surface, but the composition of other tissues differed significantly. Tm implants had more bone marrow

Table 3 Migration of polyethylene (PE) particles in all zones (total interface) in the peri-implant tissue and inside the implant coating

Particle migration in peri-implant tissue		Surgical technique			
		Exact fit	p value	Peri-implant gap	p value
Median grade	Gb implants	3 (1–4)	0.07	3 (2–4)	0.047
	Tm implants	1 (1–2)		1 (1–1)	
Particle migration inside coating					
Median grade	Gb implants	–		–	
	Tm implants	1 (1–2)		1.5 (1–2)	

Median values with interquartile range. – = not rated for Gb implants
Wilcoxon signed rank sum test
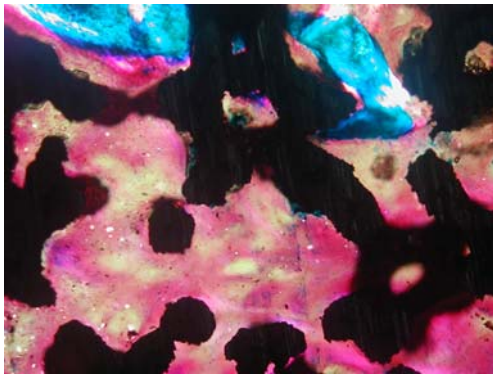
Fig. 3 The inside of a Tm implant inserted with a peri-implant gap. There was ingrowth of bone from the periphery of the implant, but most pores were filled with fibrous tissue. This section was viewed with polarised light and birefringent PE particles were seen distributed in the fibrous tissue inside the pores

(72 [56–76]%) than Gb implants (20 [13–37]%)(p=0.02) and less fibrous tissue (p=0.02; Table 2).

Implants inserted with gap

All Gb implants inserted with a gap were completely covered by fibrous tissue (Fig. 2d). This was in contrast to Tm implants where all implants had over 8% bone ongrowth (p=0.02; Fig. 2c, Table 1). Surprisingly, Tm implants inserted with a gap had significantly higher ongrowth of bone than Gb implants inserted as an exact fit (p=0.03). The volume of fibrous tissue in the initial peri-implant gap was significantly less around Tm implants than around Gb implants (Table 2).

Migration of PE particles

Significantly less PE particles were found around Tm implants than around Gb implants when inserted with a peri-implant gap. A similar difference was found for implants inserted as an exact fit; however, this was not significant (Table 3).

Owing to the nature of the implants, it was only possible to measure the number of particles inside the pores of the Tm implants. PE particles migrated inside the Tm coating of Tm implants fitted both exactly or inserted with a gap in comparable amounts (Fig. 3, Table 3).

Discussion

Wear debris and cytokines are carried by the joint fluid to the peri-implant bone in total hip replacement [25]. Once accumulated at the bone implant interface, wear particles may exhibit deleterious effects on the bone stock, either by the cellular effects of the particles alone [9, 11] or in synergy with other factors such as fluid pressure and micromotion [4, 30].

Wear particles may travel through gaps in the cement mantle, fibrous tissue or inside porous implants [1, 5]. In contrast, vital bone tissue has proven to possess a significant sealing effect against the migration of wear debris [22] and in vivo studies suggest that bone has less permeability than fibrous tissue [5, 22, 23].

In this study it was expected that the model with the highest permeability would be the highly porous Tm implant inserted with a peri-implant gap. However, this was not the case due to the superior osteoconductivity of Tm implants. The finding of PE particles inside the Tm implants in our study suggested fluid flow inside the implants. Fewer particles were found around Tm implants in exact fit but also in gap situations compared with Gb implants. However, the difference did not reach the level of significance (p=0.07) in implants fitted exactly in comparison to implants inserted leaving a gap (p=0.047).

The presence of PE particles in the pores of trabecular metal implants might be a potential risk factor for the formation of aggressive membranes inside the coating. However, the stability given by the bone ongrowth to Tm implants could significantly reduce this risk by providing a stable environment [2].

Possible explanations of the superior bone ongrowth to Tm implants could be:

1. Differences in fluid flow and pressure at the bone–implant interface
2. Increased roughness of Tm implants
3. The inter-connective porosity of Tm implants
4. Better biocompatibility of tantalum compared with Ti-6-Al-4V

Fluid flow and pressure

Clinically, intra-capsular pressure inside a hip joint with an aseptically loosened THR is elevated compared with a hip with a non-loosened implant and the pressure varies with leg position [24]. Findings of intra-articular synovitis and excess joint fluid suggested similar increased intra-articular pressure in our experimental study, where fluid and wear debris could be pumped into the implant interface and into the pores of a porous implant during joint motion. Oscillating pressure itself may have influenced the bone tissue leading to death of osteocytes and bone lysis [29, 30]. The difference in peri-implant fluid flow and pressure between Tm and Gb implants might explain that even though carefully inserted as an exact fit, Gb implants had very little bone contact after 8 weeks. The bone adjacent to the implant had been replaced by fibrous tissue covering 75% of the implant surface. In contrast, Tm implants with a 0.75 peri-implant gap had obtained significantly higher bone ongrowth than Gb implants fitted exactly. Around Gb implants inserted with a gap, bone was formed in the gap, but did not bridge it. Instead, a sclerotic bone rim was formed, which surrounded the fibrous membrane around the implant. Thus, a pathway for fluid flow and particle migration around the Gb implants was created. In contrast

the fibrous tissue and fluid flow was found inside the interconnecting pores of Tm implants. This indicated that fluid flow could continue inside the pores of Tm implants while bone formation bridged the gap around the implants. The pressure at the bone implant interface was therefore not raised to such an extent that bone formation was inhibited or osteolysis occurred, because fluid followed the path of least resistance into the implant.

Interconnectivity

Interconnectivity influences the ability of cells to proliferate and migrate through the pores and to produce mineralised bone tissue. Interconnections over 50 μm favour new bone ingrowth inside the pores and assure cell proliferation, differentiation and angiogenesis [15]. Open-pore implant coatings with interconnected structures have higher bone conductivity compared with closed-pore coatings in gap situations [23], and the results of this study confirm these findings with Tm implants having superior gap healing compared with solid implants.

Surface roughness

Differences in surface texture and thus surface roughness have been proven to influence migration of PE particles and bone ongrowth around clinical and experimental implants [5, 8]. In the present study as in previous studies, the effect of porosity or surface roughness could not be studied in isolation. However, the micro-structure of implant surfaces influences micro-environment around the implant including fluid flow and possibilities for osteoblast attachment and proliferation at the implant surface [16]. Thus, the increased roughness may have contributed to the superior bone ongrowth of Tm implants.

Biocompatibility

The biocompatibility of Ti-6-Al-4V alloy and tantalum implants used in the present study has to our knowledge not been compared previously. A study using rat bone compared the biocompatibility of commercially pure (c.p.) titanium and tantalum implants after 2 and 4 weeks. Both materials had a comparable percentage of bone contact and there were no signs of inflammation around any of the implants indicating a uniform biocompatibility of the two materials [17]. The Ti-6-Al-4V alloy used in our study may have slightly inferior biocompatibility compared with c.p. titanium [13, 28]. This cannot, however, explain the fibrous encapsulation and low percentage of bone ongrowth of Ti-6-Al-4V implants found in this study.

Conclusion

Trabecular metal implants had less migration of PE particles in peri-implant tissue than Gb implants. The sealing effect was due to superior bony gap healing and bone ongrowth to Tm implants. Possible explanations for the superior osteo-conductivity were a reduced fluid flow and pressure around the Tm implants, increased surface roughness and inter-connected porosity compared with solid titanium alloy implants.

References

1. Anthony PP, Gie GA, Howie CR, Ling RS (1990) Localised endosteal bone lysis in relation to the femoral components of cemented total hip arthroplasties. J Bone Jt Surg Br 72:971–979
2. Aspenberg P, Herbertsson P (1996) Periprosthetic bone resorption. Particles versus movement. J Bone Jt Surg Br 78:641–646
3. Baddeley AJ, Gundersen HJ, Cruz-Orive LM (1986) Estimation of surface area from vertical sections. J Microsc 142:259–276
4. Bechtold JE, Kubic V, Soballe K (2001) A controlled experimental model of revision implants. I. Development. Acta Orthop Scand 72:642–649
5. Bobyn JD, Jacobs JJ, Tanzer M, Urban RM, Aribindi R, Sumner DR, Turner TM, Brooks CE (1995) The susceptibility of smooth implant surfaces to periimplant fibrosis and migration of polyethylene wear debris. Clin Orthop Relat Res 311:21–39
6. Bobyn JD, Stackpool GJ, Hacking SA, Tanzer M, Krygier JJ (1999) Characteristics of bone ingrowth and interface mechanics of a new porous tantalum biomaterial. J Bone Jt Surg Br 81:907–914
7. Bobyn JD, Toh KK, Hacking SA, Tanzer M, Krygier JJ (1999) Tissue response to porous tantalum acetabular cups: a canine model. J Arthroplasty 14:347–354
8. Emerson RHJ, Sanders SB, Head WC, Higgins L (1999) Effect of circumferential plasma-spray porous coating on the rate of femoral osteolysis after total hip arthroplasty. J Bone Joint Surg Am 81:1291–1298
9. Goodman S, Aspenberg P, Song Y, Regula D, Lidgren L (1996) Different effects of phagocytosable particles during bone formation versus remodeling. J Biomed Mater Res 33:153–158
10. Gotfredsen K, Budtz-Jorgensen E, Jensen LN (1989) A method for preparing and staining histological sections containing titanium implants for light microscopy. Stain Technol 64:121–127

11. Green TR, Fisher J, Stone M, Wroblewski BM, Ingham E (1998) Polyethylene particles of a 'critical size' are necessary for the induction of cytokines by macrophages in vitro. Biomaterials 19:2297–2302

12. Gundersen HJ, Bendtsen TF, Korbo L, Marcussen N, Moller A, Nielsen K, Nyengaard JR, Pakkenberg B, Sorensen FB, Vesterby A et al (1988) Some new, simple and efficient stereological methods and their use in pathological research and diagnosis. Acta Pathol Microbiol Immunol Scand 96:379–394

13. Johansson CB, Han CH, Wennerberg A, Albrektsson T (1998) A quantitative comparison of machined commercially pure titanium and titanium-aluminum-vanadium implants in rabbit bone. Int J Oral Maxillofac Implants 13:315–321

14. Kim YS, Brown TD, Pedersen DR, Callaghan JJ (1995) Reamed surface topography and component seating in press-fit cementless acetabular fixation. J Arthroplasty 10:S14–S21

15. Lu JX, Flautre B, Anselme K, Hardouin P, Gallur A, Descamps M, Thierry B (1999) Role of interconnections in porous bioceramics on bone recolonization in vitro and in vivo. J Mater Sci Mater Med 10:111–120

16. Martin JY, Schwartz Z, Hummert TW, Schraub DM, Simpson J, Lankford J Jr, Dean DD, Cochran DL, Boyan BD (1995) Effect of titanium surface roughness on proliferation, differentiation, and protein synthesis of human osteoblast-like cells (MG63). J Biomed Mater Res 29:389–401

17. Matsuno H, Yokoyama A, Watari F, Uo M, Kawasaki T (2001) Biocompatibility and osteogenesis of refractory metal implants, titanium, hafnium, niobium, tantalum and rhenium. Biomaterials 22:1253–1262

18. Overgaard S, Lind M, Josephsen K, Maunsbach A, Bünger C, Søballe K (1998) Resorption of hydroxyapatite and fluorapatite ceramic coatings on weightbearing implants: a quantitative and morphological study in dogs. J Biomed Mater Res 39:141–152

19. Overgaard S, Soballe K, Gundersen G (2000) Efficiency of systematic sampling in histomorphometric bone research illustrated by hydroxyapatite-coated implants: optimizing the stereological vertical-section design. J Orthop Res 18:313–321

20. Paul HA, Bargar WL, Mittlestadt B, Musits B, Taylor RH, Kazanzides P, Zuhars J, Williamson B, Hanson W (1992) Development of a surgical robot for cementless total hip arthroplasty. Clin Orthop Relat Res 285:57–66

21. Rahbek O, Kold S, Zippor B, Overgaard S, Soballe K (2005) The influence of surface porosity on gap-healing around intra-articular implants in the presence of migrating particles. Biomaterials 26:4728–4736

22. Rahbek O, Overgaard S, Jensen TB, Bendix K, Soballe K (2000) Sealing effect of hydroxyapatite coating: a 12-month study in canines. Acta Orthop Scand 71:563–573

23. Rahbek O, Overgaard S, Lind M, Bendix K, Bunger C, Soballe K (2001) Sealing effect of hydroxyapatite coating on peri-implant migration of particles. An experimental study in dogs. J Bone Jt Surg Br 83:441–447

24. Robertsson O, Wingstrand H, Kesteris U, Jonsson K, Onnerfalt R (1997) Intracapsular pressure and loosening of hip prostheses. Preoperative measurements in 18 hips. Acta Orthop Scand 68:231–234

25. Schmalzried TP, Jasty M, Harris WH (1992) Periprosthetic bone loss in total hip arthroplasty. Polyethylene wear debris and the concept of the effective joint space. J Bone Joint Surg Am 74:849–863

26. Søballe K, Hansen ES, Rasmussen HB, Jorgensen PH, Bünger C (1992) Tissue ingrowth into titanium and hydroxyapatite-coated implants during stable and unstable mechanical conditions. J Orthop Res 10:285–299

27. Szponar B, Larsson L (2001) Use of mass spectrometry for characterising microbial communities in bioaerosols. Ann Agric Environ Med 8:111–117

28. Thompson GJ, Puleo DA (1996) Ti-6Al-4V ion solution inhibition of osteogenic cell phenotype as a function of differentiation timecourse in vitro. Biomaterials 17:1949–1954

29. Van der Vis H, Aspenberg P, de Kleine R, Tigchelaar W, Van Noorden CJ (1998) Short periods of oscillating fluid pressure directed at a titanium-bone interface in rabbits lead to bone lysis. Acta Orthop Scand 69:5–10

30. Van der Vis H, Aspenberg P, Marti RK, Tigchelaar W, Van-Noorden CJ (1998) Fluid pressure causes bone resorption in a rabbit model of prosthetic loosening. Clin Orthop Relat Res 201–208